Eight-shaped Lissajous orbits in the Earth-Moon system

Grégory Archambeau, Philippe Augros, Emmanuel Trélat

MathematicS In Action
Version de travail

Eight-shaped Lissajous orbits in the Earth-Moon system

Grégory Archambeau
Philippe Augros
Emmanuel Trélat

* EADS SPACE Transportation SAS, Flight Control Group, 66 route de Verneuil, BP 3002, 78133 Les Mureaux Cedex, France
E-mail address: gregory.archambeau@space.eads.net
† EADS SPACE Transportation SAS, Flight Control Group, 66 route de Verneuil, BP 3002, 78133 Les Mureaux Cedex, France
E-mail address: philippe.augros@space.eads.net
‡ Université d'Orléans, Laboratoire MAPMO, CNRS, UMR 6628, Fédération Denis Poisson, FR 2964, Bat. Math., BP 6759, 45067 Orléans cedex 2, France
E-mail address: emmanuel.trelat@univ-orleans.fr.

Abstract. Euler and Lagrange proved the existence of five equilibrium points in the circular restricted three-body problem. These equilibrium points are known as the Lagrange points (Euler points or libration points) $L_1, \ldots, L_5$. The existence of families of periodic and quasi-periodic orbits around these points is well known (see [20, 21, 22, 23, 37]). Among them, halo orbits are 3-dimensional periodic orbits diffeomorphic to circles. They are the first kind of the so-called Lissajous orbits. To be selfcontained, we first provide a survey on the circular restricted three-body problem, recall the concepts of Lagrange point and of periodic or quasi-periodic orbits, and recall the mathematical tools in order to show their existence. We then focus more precisely on Lissajous orbits of the second kind, which are almost vertical and have the shape of an eight – we call them *eight-shaped Lissajous orbits*. Their existence is also well known, and in the Earth-Moon system, we first show how to compute numerically a family of such orbits, based on Linsdtedt Poincaré's method combined with a continuation method on the excursion parameter. Our original contribution is in the investigation of their specific stability properties. In particular, using local Lyapunov exponents we produce numerical evidences that their invariant manifolds share nice global stability properties, which make them of interest in space mission design. More precisely, we show numerically that invariant manifolds of eight-shaped Lissajous orbits keep in large time a structure of eight-shaped tubes. This property is compared with halo orbits, the invariant manifolds of which do not share such global stability properties. Finally, we show that the invariant manifolds of eight-shaped Lissajous orbits (viewed in the Earth-Moon system) can be used to visit almost all the surface of the Moon.

1. Introduction

In the restricted three-body problem, the existence of periodic orbits around the Lagrange points is very well known. Lyapunov orbits (planar orbits) are quite easy to compute and Richardson's work (see [37]) provides a third-order approximation of the classical halo orbits (3-dimensional orbits isomorphic to ellipses) which allows to compute families of halo orbits using a shooting method. Besides Lyapunov and halo orbits, there exist other types of periodic orbits around the Lagrange points, in particular Lissajous orbits (see [20, 21, 22, 23, 24, 25]). Among those periodic orbits, we focus here on the Lissajous periodic orbits of the second kind, that are almost vertical and have the shape of an eight, and that we call *eight-shaped Lissajous orbits*. In the first part of this article, we report on the circular restricted three-body problem, recall the main underlying mathematical issues of dynamical systems theory, and then explain how to compute families of eight-shaped Lissajous orbits using a Newton's method that we combine with a continuation method on the excursion parameter. A third-order approximation of eight-shaped

The PhD of Grégory Archambeau was supported by a research contract with EADS.
Keywords: Lagrange points, Lissajous orbits, stability, mission design.
Math. classification: 70F07, 37N05.

Lissajous orbits is calculated using Linstedt Poincaré's method, which is used as an initial guess. The first part of this article (Sections 1 and 2) presents known results, and can be seen as a survey whose goal is to provide a selfcontained article. Our original contribution is mainly in the second part of the work (Section 3), in which stability properties of invariant manifolds of eight-shaped Lissajous orbits are studied and compared to the ones of halo orbits. Using local Lyapunov exponents, we prove that invariant manifolds of eight-shaped Lissajous orbits share strong global stability properties which make them of great interest in mission design analysis. Finally, to provide a relevant example of their applicability, we investigate the accessibility to the Moon surface exploration using eight-shaped Lissajous manifolds.

1.1. **Recalls on the circular restricted three-body problem**

The circular restricted three-body problem concerns the movement of a body P in the gravitational field of two masses m_1 and m_2, where the mass of P is negligible with respect to m_1 and m_2. The masses m_1 and m_2 (with $m_1 \geq m_2$) are called the primaries and are assumed to have circular coplanar orbits with the same period around their center of mass. In this problem, the influence of any other body is neglected. If the body P is further restricted to move in the plane of the two primaries, the problem is then called planar circular restricted three-body problem.

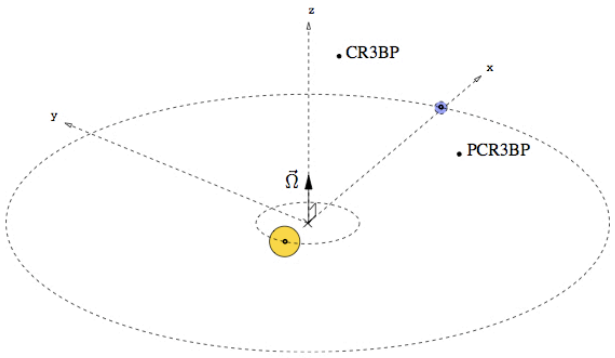

Figure 1. The restricted three-body problem

In the solar system it happens that the circular restricted three-body problem provides a good approximation for studying a large class of problems. In our application, the Earth-Moon system shall be considered. Thus, the primaries are the Earth and the Moon and gravitational forces exerted by any other planet or any other body are neglected.

In an inertial frame, the primaries positions and the equations of motion of P are time-dependent. It is thus standard to derive the equations of motion of P in a rotating frame whose rotation speed is equal to the rotation speed of the primaries around their center of mass, and whose origin is in the orbital plane of the masses m_1 and m_2. In such a frame, the positions of m_1 and m_2 are fixed. We consider the rotating frame with the x axis on the m_1-m_2 line and with origin at the libration point under consideration. The masses m_1 and m_2 move in the xy plane and the z axis is orthogonal to this plane. In addition, we use an adimensional unit system with the following agreements: the distance between the Lagrange point under consideration and the closer primary is equal to 1; the sum of the masses m_1 and m_2 is equal to 1; the angular velocity of the primaries is equal to 1. The body is submitted to the gravitational attraction forces exerted by the primaries, the Coriolis force and the centrifugal force. Let

$$X = (x, y, z, \dot{x}, \dot{y}, \dot{z})^T = (x_1, x_2, x_3, x_4, x_5, x_6)^T$$

denote the position and velocity vector of P in the rotating frame. The equations of motion are

$$\ddot{x} - 2\dot{y} = \frac{\partial \Phi}{\partial x}, \qquad \ddot{y} + 2\dot{x} = \frac{\partial \Phi}{\partial y}, \qquad \ddot{z} = \frac{\partial \Phi}{\partial z} \tag{1.1}$$

where

$$\Phi(x, y, z) = \frac{x^2 + y^2}{2} + \frac{1-\mu}{r_1} + \frac{\mu}{r_2} + \frac{\mu(1-\mu)}{2},$$

$$r_1 = \sqrt{(x+\mu)^2 + y^2 + z^2}, \qquad r_2 = \sqrt{(x-1+\mu)^2 + y^2 + z^2},$$

and $x = x_1$ and $y = x_2$ are the abscisses of the primaries m_1 and m_2. Recall that these equations have a trivial first integral, called Jacobi integral,

$$J = x^2 + y^2 + 2\frac{1-\mu}{r_1} + 2\frac{\mu}{r_2} + \mu(1-\mu)) - (\dot{x}^2 + \dot{y}^2 + \dot{z}^2),$$

related to the energy. Hence, if an energy level is fixed then the solutions live in a 5-dimensional energy manifold. The study of that manifold determines the so-called Hill's region of possible motions (see e.g. [26]).

The Lagrange points are the equilibrium points of the circular restricted three-body problem. Euler [13] and Lagrange [27] proved the existence of five equilibrium points: three collinear points on the axis joining the center of the two primaries, generally noted L_1, L_2 and L_3, and two equilateral points noted L_4 and L_5 (see Figure 2).

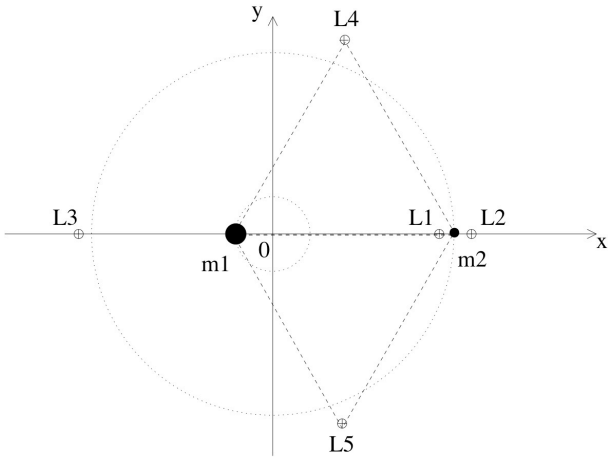

FIGURE 2. Lagrange points

For a precise computation of the Lagrange points we refer the reader to [38] (see also [26]). We recall that the collinear points are shown to be unstable (in every system), whereas L_4 and L_5 are proved to be stable under some conditions (see [32]). Actually, it follows from a generalization of a theorem of Lyapunov (due to Moser [34]) that, for a value of the Jacobi integral a bit less than the one of the Lagrange points, the solutions of the nonlinear system have the same qualitative behavior as the solutions of the linearized system, in the vicinity of the Lagrange points.

Let us focus on the three collinear Lagrange points. It is standard to expand the nonlinear terms $\frac{1}{r_1}$ and $\frac{1}{r_2}$ as series in Legendre polynomials, using the formula

$$\frac{1}{\sqrt{(x-A)^2 + (y-B)^2 + (z-C)^2}} = \frac{1}{D} \sum_{n=0}^{+\infty} \left(\frac{\rho}{D}\right)^n P_n\left(\frac{Ax + By + Cz}{D\rho}\right),$$

where $D^2 = A^2 + B^2 + C^2$ and $\rho = x^2 + y^2 + z^2$, and the equations of motion (1.1) around the libration points L_i, $i = 1, 2, 3$, can be written as

$$\begin{aligned} \ddot{x} - 2\dot{y} - (1 + 2c_2)x &= \frac{\partial}{\partial x} \sum_{n \geq 3} c_n \rho^n P_n \left(\frac{x}{\rho} \right), \\ \ddot{y} + 2\dot{x} + (c_2 - 1)x &= \frac{\partial}{\partial y} \sum_{n \geq 3} c_n \rho^n P_n \left(\frac{x}{\rho} \right), \\ \ddot{z} + c_2 z &= \frac{\partial}{\partial z} \sum_{n \geq 3} c_n \rho^n P_n \left(\frac{x}{\rho} \right), \end{aligned} \tag{1.2}$$

where

$$c_n = \frac{1}{\gamma_i^{(n+1)}} \left(\mu + \frac{(1-\mu)\gamma_i^{(n+1)}}{(1-\gamma_i)^{(n+1)}} \right).$$

Here, γ_i denotes the distance between the Lagrange point L_i and the second primary.

At the Lagrange points L_1, L_2, L_3, the linearized system consists of the linear part of equations (1.2), that is,

$$\begin{aligned} \ddot{x} - 2\dot{y} - (1 + 2c_2)x &= 0, \\ \ddot{y} + 2\dot{x} + (c_2 - 1)x &= 0, \\ \ddot{z} + c_2 z &= 0. \end{aligned} \tag{1.3}$$

It is of the kind saddle×center×center, with eigenvalues $(\pm\lambda, \pm i\omega_p, \pm i\omega_v)$, where

$$\lambda^2 = \frac{c_2 - 2 + \sqrt{9c_2^2 - 8c_2}}{2}, \quad \omega_p^2 = \frac{2 - c_2 + \sqrt{9c_2^2 - 8c_2}}{2}, \quad \omega_v^2 = c_2.$$

Lyapunov-Poincaré's Theorem implies the existence of a two-parameter family of periodic trajectories around each point (see [32], or see for instance [6]). One can also see this two-parameter family as two one-parameter families of periodic orbits. Halo orbits are periodic orbits around the Lagrange points, which are diffeomorphic to circles (see [7]). Their interest for mission design was first pointed out by Farquhar (see [14, 16]). Other families of periodic orbits, called Lissajous orbits, have been identified and computed in [20], as well as quasi-periodic orbits (see [21]). Halo orbits can be seen as Lissajous orbits of the first kind, and in the present article we focus on Lissajous orbits of the second kind, diffeomorphic to eight-shaped curves. In Section 2 we recall how to prove their existence and explain a way to compute them.

Given a periodic orbit around a Lagrange point, the stable (resp. unstable) manifold of this orbit is defined as the submanifold of the phase space consisting of all points whose future (resp. past) semi-orbits converge to the periodic orbit (such orbits are said asymptotic). It is well known that invariant manifolds of Lissajous orbits act as separatrices in the following sense (see [19]): invariant manifolds can be seen as 4-dimensional tubes, topologically equivalent to $S^3 \times \mathbb{R}$, in the 5-dimensional energy manifold mentioned previously. Due to this dimension feature, it happens that they separate two kinds of orbits, called transit orbits and non-transit orbits. The transit orbits are defined as orbits passing from one region to another, inside the 4-dimensional tubes. The non-transit orbits are outside the tubes.

2. Eight-shaped Lissajous orbits

2.1. Periodic solutions of the linearized equations

Let us first investigate the solutions of the linearized system (1.3) around L_i, for $i = 1, 2, 3$. If the initial conditions are restricted to non divergent modes, the bounded solutions of the linear

system are written as

$$\begin{array}{rcl} x(t) & = & -A_x \cos(\omega_p t + \phi), \\ y(t) & = & \kappa A_y \sin(\omega_p t + \phi), \\ z(t) & = & A_z \cos(\omega_v t + \psi), \end{array} \tag{2.1}$$

where

$$\kappa = \frac{w_p^2 + 1 + c_2}{2\omega_p} = \frac{2\lambda}{\lambda^2 + 1 - c_2},$$

and A_x, A_y and A_z are generally referred to as the x-excursion, y-excursion and z-excursion. One can immediately observe that the bounded solutions of the linear system are periodic if the in-plane and the out-of-plane frequencies, ω_p and ω_v, have a rational ratio.

Moser's Theorem mentioned previously implies that bounded trajectories can also be found for the nonlinear system. They can be seen as perturbations of the bounded trajectories of the linear system, the nonlinear terms acting on the amplitudes and the frequencies. This change of frequencies induced by the nonlinearities has been used by Richardson to calculate an approximation of halo orbits (see [37]). In the next section we use this strategy to calculate an approximation of eight-shaped Lissajous orbits.

In the expression of the bounded solutions of the linear system, the values of the frequencies ω_p and ω_v are naturally determined from the system and the libration point under consideration. But, as explained before, these eigenfrequencies change for the nonlinear system. If the nonlinearities generate equal frequencies $\omega_p = \omega_v$, then halo orbits are obtained. This was the method used by Richardson to calculate an approximation of halo orbits. Similarly, Lissajous orbits can be obtained whenever the quotient of the two eigenfrequencies is rational but different of 1 (see [20, 21]).

2.2. **Lindstedt Poincaré's method**

To calculate approximations of periodic solutions around the libration points, we use Lindstedt-Poincaré's method, based on the vision that the nonlinearities change the solutions of the linearized system by changing their eigenfrequencies. This method is well known and has been very well surveyed e.g. in [31]. The idea is that periodic or quasi-periodic solutions of the linearized system (1.3) are characterized by an harmonic motion in the so-called in-plane (xy) with a certain period, and an oscillation in the so-called out-of-plane z direction with another possible period. For instance, to compute periodic halo orbits, one imposes that both periods coincide. To compute planar and vertical Lyapunov families of periodic orbits, it suffices to take one of the two amplitudes equal to zero; notice that these families of Lyapunov orbits tend to the libration point whenever the amplitude tends to zero (see [31] and references therein for more details).

Here, since we aim at computing an eight-shaped Lissajous orbit, we consider a nominal eight-shaped orbit, with frequencies ω_p and ω_v satisfying $\omega_v = \frac{\omega_p}{2}$. With such values, the linearized equations are written as

$$\begin{array}{l} \ddot{x} - 2\dot{y} - (1 + 2c_2)x = 0, \\ \ddot{y} + 2\dot{x} + (c_2 - 1)y = 0, \\ \ddot{z} + \left(\frac{\omega_p}{2}\right)^2 z = 0, \end{array} \tag{2.2}$$

and have periodic orbits parametrized by

$$\begin{array}{rcl} x(t) & = & -A_x \cos(\omega_p t + \phi), \\ y(t) & = & \kappa A_y \sin(\omega_p t + \phi), \\ z(t) & = & A_z \cos(\frac{\omega_p}{2} t + \psi), \end{array} \cdot \tag{2.3}$$

which are eight-shaped, diffeomorphic to the solution drawn on Figure 3.

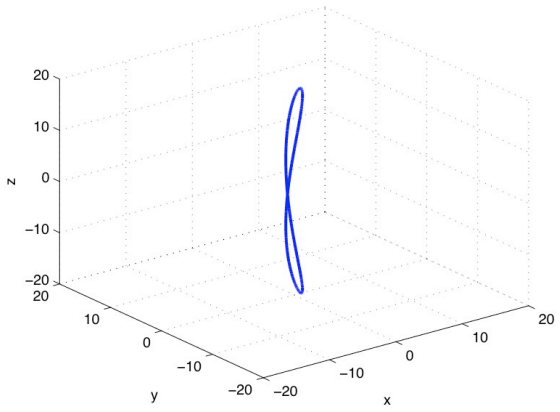

Figure 3. Representation of the curve $x(t) = \cos(2t)$, $y(t) = \sin(2t)$, $z(t) = 20\cos(t)$, where $t \in [0, 2\pi]$.

Imposing $\omega_v = \frac{\omega_p}{2}$ in the equations of motion (1.2) leads to

$$\begin{aligned} \ddot{x} - 2\dot{y} - (1+2c_2)x &= \frac{\partial}{\partial x}\sum_{n\geq 3} c_n \rho^n P_n\left(\frac{x}{\rho}\right), \\ \ddot{y} + 2\dot{x} + (c_2 - 1)y &= \frac{\partial}{\partial y}\sum_{n\geq 3} c_n \rho^n P_n\left(\frac{x}{\rho}\right), \\ \ddot{z} + \left(\frac{\omega_p}{2}\right)^2 z &= \frac{\partial}{\partial z}\sum_{n\geq 3} c_n \rho^n P_n\left(\frac{x}{\rho}\right) + \Delta z, \end{aligned} \tag{2.4}$$

where $\Delta = (\frac{\omega_p}{2})^2 - \omega_v^2$. In such a way, the reference orbit of the Linsdtedt-Poincaré's method is enforced to an eight-shaped orbit. Then, to take into account the fact that the nonlinearities change the eigenfrequencies, the Linsdtedt-Poincaré's method consists in considering time-varying frequencies in the following way. Set $\tau = \nu t$, and consider the corrected frequency

$$\nu = 1 + \sum_{n\geq 1} \nu_n, \quad \nu_n < 1.$$

The method consists in tuning iteratively the parameters ν_n so as to filter out all secular terms appearing in the expansion of the solution and causing a blow up. Let us introduce several notations and assumptions. First, for every integer p and all elements v and w of $\mathbb{R}^p$, of coordinates in the canonical basis of $\mathbb{R}^p$,

$$v = \begin{pmatrix} v_1 \\ v_2 \\ \vdots \\ v_p \end{pmatrix} \quad \text{and} \quad w = \begin{pmatrix} w_1 \\ w_2 \\ \vdots \\ w_p \end{pmatrix},$$

define $v \cdot *w \in \mathbb{R}^p$ as the vector

$$v \cdot *w = \begin{pmatrix} v_1 w_1 \\ v_2 w_2 \\ \vdots \\ v_p w_p \end{pmatrix}.$$

With this notation, the reference solution is written as

$$q_{ref}(\tau) = \begin{pmatrix} A_x \\ A_x \\ A_z \end{pmatrix} \cdot * \begin{pmatrix} -\cos(\omega_p \tau + \phi) \\ \kappa \sin(\omega_p \tau + \phi) \\ \sin(\frac{\omega_p}{2}\tau + \psi) \end{pmatrix} = \bar{A} \cdot * q_0(\tau).$$

The reference solution being considered as the first term of a series expansion, it is natural to seek a periodic solution in the form of a series in $\bar{A}$,

$$q(\tau) = \begin{pmatrix} x(\tau) \\ y(\tau) \\ z(\tau) \end{pmatrix} = \bar{A} \cdot * q_0 + \bar{A}^2 \cdot * q_1 + \bar{A}^3 \cdot * q_2 + \ldots = \begin{pmatrix} Ax_0(\tau) + A^2 x_1(\tau) + A^3 x_2(\tau) + \ldots \\ Ay_0(\tau) + A^2 y_1(\tau) + A^3 y_2(\tau) + \ldots \\ Az_0(\tau) + A^2 z_1(\tau) + A^3 z_2(\tau) + \ldots \end{pmatrix} \tag{2.5}$$

where A^n denotes the two-variables polynomial of degree n

$$A^n = \sum_{\substack{l,p=1 \\ l+p=n}}^{n} \lambda_{l,p} A_x^l A_z^p.$$

Note that considering an n-th-order approximation of the solution amounts to truncating the series expansion at order n. Finally, the ν_n are assumed to have the same order as A^n. We next rewrite the equations of motion in terms of these variables,

$$\begin{aligned} \nu^2 \ddot{x} - 2\nu\dot{y} - (1 + 2c_2)x &= \frac{3}{2}(2x^2 - y^2 - z^2) + 2c_4 x(2x^2 - 3y^2 - 3z^2) + 0(4), \\ \nu^2 \ddot{y} + 2\nu\dot{x} + (c_2 - 1)y &= -3c_3 xz - \frac{3}{2}c_4 y(4x^2 - y^2 - z^2) + 0(4), \\ \nu^2 \ddot{z} + (\frac{\omega_p}{2})^2 z &= -3c_3 xz - \frac{3}{2}c_4 z(4x^2 - y^2 - z^2) + \Delta z + 0(4), \end{aligned} \tag{2.6}$$

where the remainder term $O(4)$ contains terms of order greater than or equal to 4. Then, plugging the series expansion (2.5) into (2.6), one gets:

- at the first order in A:

$$\begin{aligned} A_x \ddot{x}_0 - 2A_x \dot{y}_0 - (1 + 2c_2)A_x x_0 &= 0, \\ A_x \ddot{y}_0 + 2A_x \dot{x}_0 + (c_2 - 1)A_x y_0 &= 0, \\ A_z \ddot{z}_0 + A_z (\frac{\omega_p}{2})^2 z_0 &= 0; \end{aligned}$$

- at the second order in A:

$$\begin{aligned} A^2 \ddot{x}_1 - 2A^2 \dot{y}_1 - (1 + 2c_2)A^2 x_1 &= -2\nu_1 A_x \ddot{x}_0 + 2\nu_1 A_x \dot{y}_0 \\ &\quad + \frac{3}{2}\left(2A_x^2 x_0^2 - A_x^2 y_0^2 - A_z^2 z_0^2\right), \\ A^2 \ddot{y}_1 + 2A^2 \dot{x}_1 + (c_2 - 1)A^2 y_1 &= -2\nu_1 A_x \ddot{y}_0 - 2\nu_1 A_x \dot{x}_0 - 3c_3 A_x^2 x_0 y_0, \\ A^2 \ddot{z}_1 + (\frac{\omega_p}{2})^2 A^2 z_1 &= -2\nu_1 A_z \ddot{z}_0 - 3c_3 A_x A_z x_0 z_0; \end{aligned}$$

- at the third order in A:

$$\begin{aligned}
A^3\ddot{x}_2 - 2A^3\dot{y}_2 - (1+2c_2)A^3x_2 &= -2\nu_1A^2\ddot{x}_1 - (\nu_1+2\nu_2)A_x\ddot{x}_0 + 2\nu_1A^2\dot{y}_1 \\
&\quad +2A^3\dot{y}_2 + 2\nu_2A_x\dot{y}_0, \\
A^3\ddot{y}_2 + 2A^3\dot{x}_2 + (c_2-1)A^3y_2 &= -2\nu_1A^2\ddot{y}_1 - 2\nu_1A^2\dot{x}_1 - (\nu_1^2+2\nu_2)A_x\ddot{y}_2 \\
&\quad -2\nu_2A_x\dot{x}_0 - 3c_3(A_xA^2x_0y_1 + A_xA^2y_0x_1) \\
&\quad -\frac{3}{2}c_4A_xy_0(4A_x^2x_0^2 - A_x^2y_0^2 - A_z^2z_0^2), \\
A^3\ddot{z}_2 + (\frac{\omega_p}{2})^2A^3z_2 &= -2\nu_1A^2\ddot{z}_1 - (\nu_1^2+2\nu_2)A_z\ddot{z}_0 \\
&\quad -3c_3(A_xA^2x_0z_1 + A_zA^2x_1z_0) + \Delta A_zz_0.
\end{aligned}$$

The Lindstedt-Poincaré's method now consists in determining the coefficients ν_n in function of A_x and A_z so as to filter out the secular terms that appear in the expansion of the solution. At the first order in A, we recover the expected solution

$$\begin{pmatrix} x_0(\tau) \\ y_0(\tau) \\ z_0(\tau) \end{pmatrix} = \begin{pmatrix} -\cos(\omega_p\tau+\phi) \\ \kappa\sin(\omega_p\tau+\phi) \\ \sin(\frac{\omega_p}{2}\tau+\psi) \end{pmatrix}.$$

At the second order in A, the equations in x and y are decoupled from the equation in z, and it is possible to choose ν_1 so as to filter out the possible secular terms that appear whenever modes of the second member of the differential equation coincide with modes of the first member. In our case, the modes of the equation without second member remain the same, that is $(\pm\lambda, \pm i\omega_p)$. As a consequence, in the right-hand side, terms of frequency ω_p must be cancelled. The terms in x_0^2, y_0^2, z_0^2 and x_0z_0 do not raise any problem since they are linearized into $1, \cos(2\omega_p\tau), \sin(2\omega_p\tau)$. The terms $\ddot{x}_0$, $\ddot{y}_0$, $\dot{x}_0$ and $\dot{y}_0$ are linearized into $\cos(\omega_p\tau)$ and $\sin(\omega_p\tau)$ and may generate secular terms. Since ν_1 appears as a multiplicative scalar factor of those terms, it suffices to choose $\nu_1 = 0$ to cancel secular terms. With this choice of ν_1, the resulting differential equation is written as

$$\begin{aligned}
A^2\ddot{x}_1 - 2A^2\dot{y}_1 - (1+2c_2)A^2x_1 &= \frac{3}{2}(2A_x^2x_0^2 - A_x^2y_0^2 - A_z^2z_0^2), \\
A^2\ddot{y}_1 + 2A^2\dot{x}_1 + (c_2-1)A^2y_1 &= -3c_3A_x^2x_0y_0,
\end{aligned}$$

and can be solved explicitly. We get

$$A^2\begin{pmatrix} x_1(\tau) \\ y_1(\tau) \\ z_1(\tau) \end{pmatrix} = \begin{pmatrix} a_{21}A_x^2 + a_{22}A_z^2 + (a_{23}A_x^2 - a_{24}A_z^2)\cos(2\omega_p\tau+\phi) \\ (b_{21}A_x^2 - b_{22}A_z^2)\sin(2\omega_p\tau+\phi) \\ \delta_r d_{21}A_xA_z(\cos(2\frac{\omega_p}{2}\tau+\psi) - 3) \end{pmatrix},$$

with $\delta_r = 2 - r$, where r characterizes the class of the orbit and in particular its direction of rotation ($r = 1$ for a first class orbit and $r = 3$ for a second class orbit).

Then, the next step consists in plugging the obtained expressions of x_1, y_1 into the equations in x and y at the third order, and to determine the parameter ν_2 so as to filter out the possible secular terms. Easy calculations show that one must choose

$$\nu_2 = s_1A_x^2 + s_2A_z^2,$$

where

$$\begin{aligned}
s_1 &= \frac{\frac{3}{2}c_3(2a_{21}(\kappa^2-2) - a_{23}(\kappa^2+2) - 2\kappa b_{21}) - \frac{3}{8}(3\kappa^4 - 8\kappa^2 + 8)}{2\lambda(\lambda(1+\kappa^2) - 2\kappa)}, \\
s_2 &= \frac{\frac{3}{2}c_3(2a_{22}(\kappa^2-2) - a_{24}(\kappa^2+2) + 2\kappa b_{22} + 5d_{21}) + \frac{3}{8}c_4(12-\kappa^2)}{2\lambda(\lambda(1+\kappa^2) - 2\kappa)},
\end{aligned}$$

where $\kappa = \frac{1}{2\lambda}(\lambda^2 + 1 + 2c_2)$, and λ is solution of $\lambda^4 + (c_2 - 2)\lambda^2 - (c_2 - 1)(1 + 2c_2) = 0$. The coefficients a_{ij}, b_{ij} and d_{ij} are given by

$$\begin{aligned}
a_{21} &= \frac{3c_3(\kappa^2 - 2)}{4(1 + 2c_2)}, \quad a_{22} = \frac{3c_3}{4(1 + 2c_2)}, \\
a_{23} &= -\frac{3c_3\lambda}{4\kappa d_1}[3\kappa^3\lambda - 6\kappa(\kappa - \lambda) + 4], \quad a_{24} = -\frac{3c_3\lambda}{4\kappa d_1}(2 + 3\kappa\lambda), \\
a_{31} &= -\frac{9\lambda}{4d_2}(4c_3(\kappa a_{23} - b_{21}) + \kappa c_4(4 + \kappa^2)) \\
&\quad + \left(\frac{9\lambda^2 + 1 - c_2}{2d_2}\right)\left(3c_3(2a_{23} - \kappa b_{21}) + c_4(2 + 3\kappa^2)\right), \\
a_{32} &= -\frac{1}{d^2}\Big(\frac{9\lambda}{4}\left(4c_3(\kappa a_{24} - b_{22}) + \kappa c_4\right) \\
&\qquad + \frac{3}{2}(9\lambda^2 + 1 - c_2)\left(c_3(\kappa b_{22} + d_{21} - 2a_{24}) - c_4\right)\Big), \\
b_{21} &= -\frac{3c_3\lambda}{2d_1}(3\kappa\lambda - 4), \quad b_{22} = \frac{3c_3\lambda}{d_1}, \\
b_{31} &= \frac{3}{8d_2}\Big(8\lambda\left(3c_3(\kappa b_{21} - 2a_{23}) - c_4(2 + 3\kappa^2)\right) \\
&\qquad + (9\lambda^2 + 1 + 2c_2)\left(4c_3(\kappa a_{23} - b_{21}) + \kappa c_4(4 + \kappa^2)\right)\Big), \\
b_{32} &= \frac{1}{d_2}\Big(9\lambda\left(3c_3(\kappa b_{22} + d_{21} - 2a_{24}) - c_4\right) \\
&\qquad + \frac{3}{8}(9\lambda^2 + 1 + 2c_2)\left(4c_3(\kappa a_{24} - b_{22}) + \kappa c_4\right)\Big), \\
d_{21} &= -\frac{c_3}{2\lambda^2}, \quad d_{31} = \frac{3}{64\lambda^2}(4c_3a_{24} + c_4), \\
d_{32} &= \frac{3}{64\lambda^2}\left(4c_3a_{23} - d_{21} + c_4(4 + \kappa^2)\right),
\end{aligned}$$

with $d_1 = \frac{3\lambda^2}{\kappa}\left(\kappa(6\lambda^2 - 1) - 2\lambda\right)$ and $d_2 = \frac{8\lambda^2}{\kappa}\left(\kappa(11\lambda^2 - 1) - 2\lambda\right)$.

Secular terms appearing in the third-order equation in z cannot be removed by choosing a coefficient ν_i as previously. It is necessary to specify amplitude and phase angle constraint relationships in order to filter out these secular terms. The amplitude constraint relationship is

$$l_1A_x^2 + l_2A_z^2 + \Delta = 0,$$

where $l_1 = a_1 + 2l^2s_1$ and $l_2 = a_2 + 2l^2s_2$, with $a_1 = -\frac{3}{2}c_3(2a_{21} + a_{23} + 5d_{21}) - \frac{3}{8}c_4(12 - k^2)$ and $a_2 = \frac{3}{2}(a_{24} - 2a_{22}) + \frac{9}{8}c_4$, and the phase angle constraint relationship is

$$\psi = \phi + \frac{r\pi}{2}, \quad r = 1, 3.$$

Note that the formulas defining the coefficients l_i, $a_{i,j}$, $b_{i,j}$ and d_{ij} are the same as the ones obtained by Richardson in [37] to determine a third-order approximation of the halo orbits. With these relations, calculations lead to

$$A^3\begin{pmatrix} x_2(\tau) \\ y_2(\tau) \\ z_2(\tau) \end{pmatrix} = \begin{pmatrix} (a_{31}A_x^3 - a_{32}A_xA_z^2)\cos(3\omega_p\tau + \phi) \\ (b_{31}A_x^3 - b_{32}A_xA_z^2)\sin(3\omega_p\tau + \phi) \\ \delta_r(d_{32}A_zA_x^2 - d_{31}A_z^3)\cos(3\frac{\omega_p}{2}\tau + \psi) \end{pmatrix}.$$

Finally, we arrive at the following third-order approximation of eight-shaped Lissajous orbits:

$$\begin{aligned} x &= a_{21}A_x^2 + a_{22}A_z^2 - A_x\cos(\tau_1) + (a_{23}A_x^2 - a_{24}A_z^2)\cos(2\tau_1) \\ &\quad +(a_{31}A_x^3 - a_{32}A_xA_z^2)\cos(3\tau_1), \\ y &= kA_x\sin(\tau_1) + (b_{21}A_x^2 - b_{22}A_z^2)\sin(2\tau_1) + (b_{31}A_x^3 - b_{32}A_xA_z^2)\sin(3\tau_1), \\ z &= \delta_r A_z\cos(\tau_2) + \delta_n d_{21}A_xA_z(\cos(2\tau_2) - 3) + \delta_n(d_{32}A_zA_x^2 - d_{31}A_z^3)\cos(3\tau_2), \end{aligned}$$

where $\tau_1 = \omega_p\tau + \phi$ and $\tau_2 = \frac{\omega_p}{2}\tau + \psi$. These formulas provide an approximation of possible initial points of eight-shaped Lissajous orbits, parametrized by their z-excursion A_z. As we will see in the next section, these third-order approximations are satisfactory for small values of A_z but are not precise enough for larger values, and we will use a continuation method to compute our periodic orbits.

2.3. **Computation of a family of eight-shaped Lissajous orbits**

In the previous section, a third-order approximation of eight-shaped Lissajous periodic orbits has been calculated analytically. In this section we show how to compute a family of eight-shaped Lissajous orbits, parametrized by the z-excursion A_z. The previous third-order approximation of those orbits, used as an initial guess in a Newton-like procedure, permits to compute some eight-shaped Lissajous orbits for small values of A_z but is not precise enough to initialize successfully the Newton method for larger values. To overcome this problem, one may then try to derive an approximation of larger order, so as to get a more precise initial guess, in the hope that it will suffice to make converge the Newton procedure (as done e.g. in [20, 21, 26, 31] where this procedure has been implemented). Instead of that, we use here a continuation method on the parameter A_z, in order to generate a family of eight-shaped Lissajous orbits. The procedure is detailed next.

We first recall how Newton's method is usually implemented to compute periodic orbits in the restricted three body problem. Notice that, if $(x(t), y(t), z(t))$ is a solution of the system, then $(x(-t), -y(-t), z(-t))$ is also solution. Using this symmetry property, the method consists in determining an adapted initial condition X_0 on the plane $y = 0$, with a velocity orthogonal to this plane, thus of the form $X_0 = (x_0, 0, z_0, 0, \dot{y}_0, 0)^T$, generating a semiorbit which reintersects the plane $y = 0$ orthogonally. Fixing the z-excursion z_0, Newton's method consists in tuning the values of the initial coordinates x_0, $\dot{y}_0$ and of the orbital period T so that the corresponding solution verifies $y(\frac{T}{2}) = \dot{x}(\frac{T}{2}) = \dot{z}(\frac{T}{2}) = 0$. This shooting method permits to reach a very good precision and is then used at every step of the iteration procedure of the continuation method described next.

Let A_z be the z-excursion of the eight-shaped Lissajous orbit to be computed, and X_0 the corresponding initial condition to be determined. If A_z^0 is the z-excursion of the first eight-shaped Lissajous orbit computed thanks to the third-order approximation, the continuation method consists in making the z-excursion vary from A_z^0 to A_z, according to an appropriate subdivision, and solving at each iteration the Newton's problem initialized with the result of the previous step. More precisely, let A_z^n be the n-th z-excursion of the subdivision. Assume that each eight-shaped Lissajous orbit has already been computed for A_z^p, $p \in 1, \ldots, n$, the resulting initial condition being noted X_0^p. In order to compute the eight-shaped Lissajous orbit of z-excursion A_z^{n+1}, the continuation method consists in using the initial condition X_0^n as a first guess for the Newton's method. If the subdivision is fine enough then the Newton's method converges to a point which is then chosen as initial guess X_0^{n+1}. The latter is used to compute the eight-shaped Lissajous orbit of z-excursion A_z^{n+1}, and the procedure goes on by iteration, until the eight-shaped Lissajous orbit of z-excursion A_z is computed. Table (1) draws a diagram of the continuation procedure.

Initial information	Newton's $\longrightarrow$ method	Numerical results
A_z^0, X_0^0	$\longrightarrow$	X_0^1
$\swarrow$	$\swarrow$	
A_z^1, X_0^1	$\longrightarrow$	X_0^2
$\swarrow$	$\swarrow$	
$\vdots$	$\vdots$	$\vdots$
$\swarrow$	$\swarrow$	
A_z^{n-1}, X_0^{n-1}	$\longrightarrow$	X_0^n
$\swarrow$	$\swarrow$	
A_z, X_0^n	$\longrightarrow$	X_0

TABLE 1. Continuation method algorithm

A single eight-shaped Lissajous orbit around Lunar L_1 (that is the Lagrange point L_1 in the Earth-Moon system) is represented on Figure 4 in position and velocity spaces.

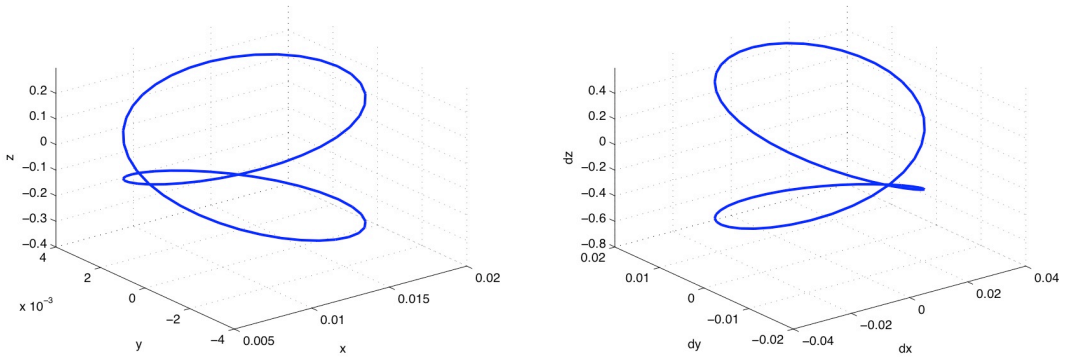

(a) (b)

FIGURE 4. (a) Eight-shaped Lissajous orbit around Lunar L_1 in the position space. (b) Eight-shaped Lissajous orbit around Lunar L_1 in the velocity space.

Figure 5 represents the projections of a family of eight-shaped Lissajous orbits on the planes (x, y), (y, z) and (x, z) computed using the continuation method.

Remark 2.1. To generate a starting point of the above computed family, we used the approximation at the third order described in the previous section. Then, the family has been generated by continuation on the excursion parameter. For the continuation method to hold, it is necessary that one does not encounter any singularity. In particular, our family must not contain any orbit of collision. Note that it is not our aim to generate exhaustive families of orbits, but rather to compute some of them and then to investigate their stability properties. Our work is prospective.

Remark 2.2. It is interesting to compare the approximations derived from the Lindstedt-Poincaré method with the continuation method. Such simulation results are reported in Table 2.3, in which the first column consists of the excursion parameters A_z of some family of eight-shaped Lissajous orbits around the Lagrange point L_2 in the Earth-Moon system, and the second (resp. the third) column reports the norm of the difference of initial points (resp. velocities) of both methods. All

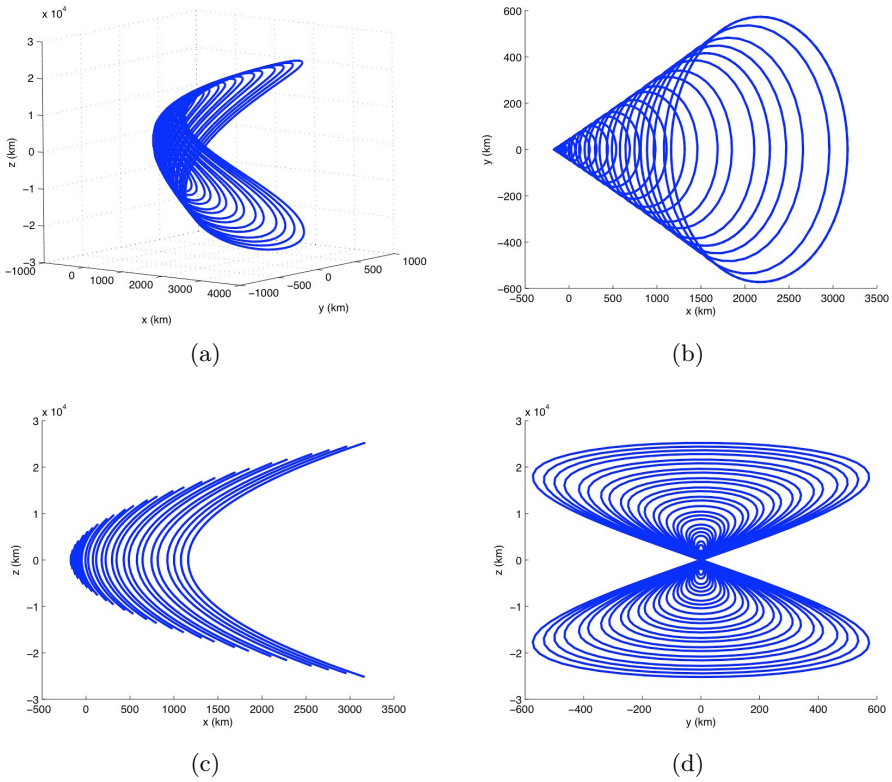

FIGURE 5. Family of eight-shaped Lissajous orbits and their projection on the (x, y), (y, z) and (x, z)-planes.

data are given in normalized units, in the sense that the distance of the point L_2 to the Moon is equal to 1, and the rotation period around the Moon is equal to 2π. We observe on this table that the precision deteriorates while A_z increases, as expected. Notice also that, when applying the Newton method with the starting point determined by the third-order Linstedt-Poincaré approximation, the method converges only for the two smallest values of the table (this means that the approximation point falls into the domain of convergence of the Newton method) and diverges for larger values.

3. Properties of invariant manifolds of eight-shaped Lissajous orbits near L_1

3.1. Empiric stability

The interest of eight-shaped Lissajous orbits is mainly in two properties shared by their invariant manifolds. The stable (resp. unstable) manifold of an eight-shaped Lissajous orbit is the submanifold of the phase space consisting of all points whose future (resp. past) semi-orbits converge to it (asymptotic orbits). Locally, in the neighborhood of a given eight-shaped Lissajous orbit, they look like eight-shaped tubes (see Figure 6).

To compute the invariant manifolds, their linear approximation is first used around periodic orbits. At each point a of a given eight-shaped Lissajous orbit Σ, one computes the eigenvectors $V^s(a)$ and $V^u(a)$ associated with the real eigenvalues of the monodromy matrix at a that are lower and greater than 1. Then, one gets an approximation of the stable and unstable manifolds by propagating the orbits solutions of the equations of motion starting from initial conditions

$$X_0 = a + \varepsilon V(a),$$

A_z	norm of the difference of initial points	norm of difference of initial velocities
00010	2.480508256e-003	2.571078939e-009
00100	3.963632986e-003	2.543435521e-007
00500	1.572915399e-002	6.357949547e-006
01000	3.116814309e-002	2.543210324e-005
02000	6.219001345e-002	1.017338378e-004
03000	9.324351620e-002	2.289214928e-004
04000	1.243040288e-001	4.070222970e-004
05000	1.553663195e-001	6.360745378e-004
06000	1.864283990e-001	9.161277288e-004
07000	2.174892057e-001	1.247242823e-003
08000	2.485480265e-001	1.629492124e-003
09000	2.796043035e-001	2.062960975e-003
10000	3.106575570e-001	2.547746083e-003
15000	4.658639258e-001	5.745728564e-003
20000	6.209357375e-001	1.024907118e-002
25000	7.758283810e-001	1.608681682e-002
30000	9.304997024e-001	2.329998323e-002
35000	1.084910366e+000	3.194329031e-002
40000	1.239024778e+000	4.208546810e-002
45000	1.392812237e+000	5.380583070e-002
50000	1.546248002e+000	6.718267632e-002
55000	1.699313566e+000	8.226533883e-002
60000	1.851994604e+000	9.901585020e-002

TABLE 2.

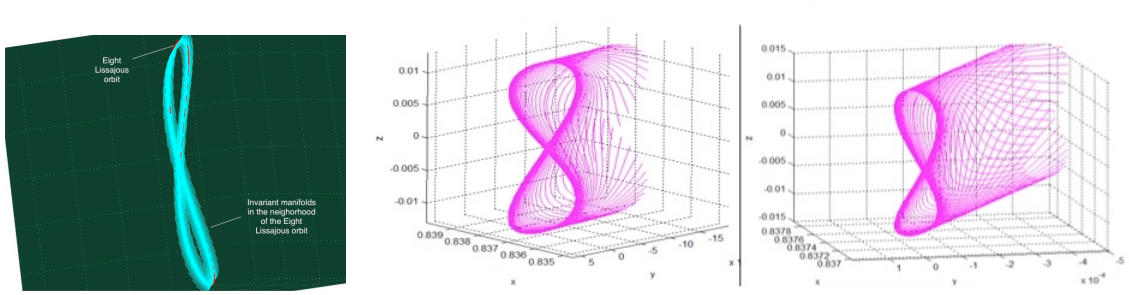

FIGURE 6. Invariant manifolds in the neighborhood of an eight-shaped Lissajous orbit

where a belongs to the eight-shaped Lissajous orbit, $V(a)$ is a normalized stable or unstable eigenvector of the monodromy matrix at a, and ε is a positive real number, small enough to ensure a good linear approximation but however not too small in order to avoid too long integration times. Indeed, the asymptotic orbits which generate the invariant manifolds rotate strongly when tending to the eight-shaped Lissajous orbit (see e.g. [26]). Some numerical results are provided on Figure 7, for the Lagrange point L_1 in the Earth-Moon system. In the sequel, all our simulations concern orbits around the Lagrange point L_1 in the Earth-Moon system. In this system, denoting by M_E the mass of the Earth and by M_M the mass of the Moon, there holds $\mu = \frac{M_M}{M_E+M_M} = 0.01215616930968$.

A first important property that we observe on the numerical simulations is that, contrarily to halo orbits, the invariant manifolds of eight-shaped Lissajous orbits seem to keep the same structure in large time. This global stability property which is numerically observed is also

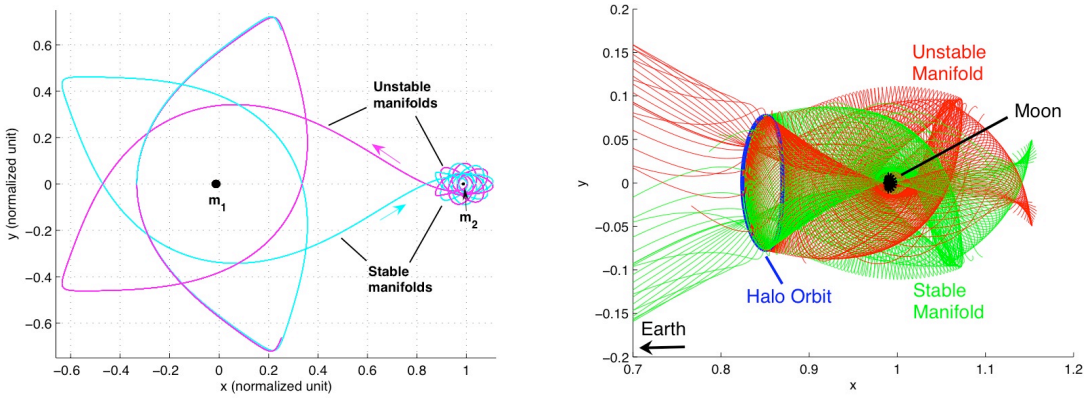

(a) Invariant manifolds of an eight-shaped Lissajous orbit

(b) Invariant manifolds of a halo orbit

Figure 7. Invariant manifolds of an eight-shaped Lissajous orbit and of a halo orbit

illustrated on Figure 8 where different images of an eight-shaped Lissajous orbit by the flow at different times are represented. These simulations were realized for a given eight-shaped Lissajous orbit of the previously computed family of orbits, and we observe on our simulations that our qualitative observations do not depend on the specific orbit that is chosen in the family.

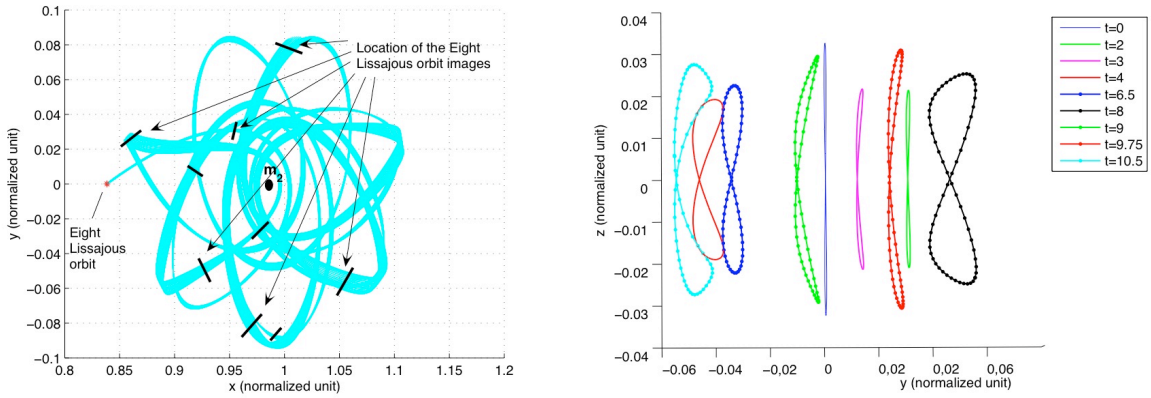

(a) Invariant manifold of an eight-shaped Lissajous orbit around the Lagrange point L_1 in the Earth-Moon system

(b) Images of the eight-shaped Lissajous orbit by the flow at different times

Figure 8.

This property is of particular interest for mission design. Note that such a stability property does not hold for halo orbits. Indeed, the invariant manifolds of a classical halo orbit have the aspect of a regular tube in the neighborhood of the orbit but this regular aspect is not persistent far away from the halo orbit and/or in large integration time; in particular these tubes behave in a chaotic way in large time. In contrast, the regular structure of invariant manifolds of eight-shaped Lissajous orbits is conserved even after a large integration time. This global stability property may be relevant for mission computation since it allows to predict the behavior of the trajectories which propagate on and inside these invariant manifolds in large time.

Remark 3.1. As pointed out by one of the reviewers, this stability property is in accordance with the fact that eight-shaped Lissajous orbits should not have any homoclinic nor heteroclinic connections (see [3]).

We next investigate in more details these stability properties of invariant manifolds of halo and eight-shaped Lissajous orbits (related to the Lagrange point L_1 of the Earth-Moon system) using Lyapunov exponents.

3.2. **Local Lyapunov Exponents**

The concept of Lyapunov exponents (or characteristic exponents) was introduced in [29] in order to investigate the stability properties of solutions of differential equations, and has been extensively used and studied in the literature. Lyapunov exponents measure the exponential convergence or divergence of nearby trajectories in a dynamical system, and provide indications on the behavior in large time of solutions under infinitesimal perturbations. A positive Lyapunov exponent means that nearby trajectories may diverge, whereas a negative Lyapunov exponent indicates a stability property. Computational issues have been studied e.g. in [10] (see also references therein). We use here this concept to investigate stability features of the invariant manifolds of eight-shaped Lissajous orbits.

First of all, recall the following general facts. Consider a nonlinear differential equation $\dot{x}(t) = f(t, x(t))$ in $\mathbb{R}^n$, with $x(0) = x_0$, where f is of class C^1. An important consequence of the seminal article [35] of Oseledec is that the Lyapunov exponents of an ergodic dynamical system do not depend on the specific trajectory; more precisely, given any invariant measure μ for the flow, they are the same for μ-almost every initial condition. Let now $x(\cdot)$ be a solution; for every $s \in \mathbb{R}$, the resolvent $t \mapsto \Phi(t, s)$ along $x(\cdot)$ (also called state transition matrix) is defined as the unique $n \times n$ matrix solution of the linearized system along $x(\cdot)$

$$\dot{Y}(t) = \frac{\partial f}{\partial x}(t, x(t)).Y(t), \quad Y(s) = I_n.$$

For every $t \geq 0$, set $\Lambda_{x_0}(t) = \Big(\Phi(t,0)^T \Phi(t,0)\Big)^{1/2t}$. Then, in the ergodic case the matrix $\Lambda = \lim_{t\to+\infty} \Lambda_{x_0}(t)$ is well defined and is symmetric positive definite, is almost everywhere independent on x_0 with respect to an ergodic measure (see [35]), and the Lyapunov exponents λ_i are defined as the logarithm of the eigenvalues μ_i of Λ; moreover, denoting v_i the eigenvectors associated to the eigenvalues μ_i, for $i = 1, \ldots, n$, one has

$$\lambda_i = \lim_{t\to+\infty} \frac{1}{t} \ln \|\Phi(t,0)v_i\|,$$

where $\|\cdot\|$ denotes the Euclidean norm. These coefficients provide an indication on how nearby trajectories of the system may converge or diverge from $x(\cdot)$. Notice that this is an ergodic result, that is valuable whenever t tends to $+\infty$: in ergodic systems, almost all trajectories yield the same Lyapunov exponents.

The situation is different if trajectories are followed in finite time. Instead of taking the limit, one defines, for $\Delta > 0$, the local Lyapunov exponent (in short, LLE)

$$\lambda(t, \Delta) = \frac{1}{\Delta} \ln \left(\text{maximal eigenvalue of } \sqrt{\Phi(t+\Delta, t)\Phi^T(t+\Delta, t)} \right). \tag{3.1}$$

Note that, if Δ tends to $+\infty$, one recovers the usual Lyapunov exponent. The parameter Δ stands for a positive duration over which the effect of some perturbations is tested. Contrarily to the Lyapunov exponents, the LLEs depend on the initial point, on the specific reference trajectory $x(\cdot)$ that is followed, and on the duration Δ. Such exponents, defined e.g. in [10, 12], give information on the nonuniform properties of the system, and provide an indication on the effect a perturbation at time t would be expected to have over a duration Δ. Large LLEs indicate that the trajectory crosses a region where the dependence with respect to initial

conditions is strong, hence the predictability of the evolution of the trajectory in such a region region is restricted. If they are small, or negative, then the predictability in this region of the space is improved. Definitions and algorithms to compute such exponents were given in [1, 5, 10, 12, 39, 40]. In [2], a stability technique based on local Lyapunov exponents is applied for maneuver design and navigation in the three-body problem. It is shown in [9] that finite-time Lyapunov exponents can provide useful information on the qualitative behavior of trajectories in the context of astrodynamics. Local Lyapunov exponents are used to determine the behavior of nearby trajectories in finite time. They provide indications on the effects that perturbations or maneuvers will have on trajectories over a certain period of time. In the case of the circular restricted three-body problem, which is known to be chaotic, local Lyapunov exponents cannot be expected to be negative. It is however interesting to compute local Lyapunov exponents in our study to measure the stability of eight-shaped Lissajous orbits and of their invariant manifolds, and compare them with the ones of classical halo orbits and of their invariant manifolds.

When Δ is large, the eigenvectors of the matrix $\sqrt{\Phi(t+\Delta,t)\Phi^T(t+\Delta,t)}$ tend to align along the eigenspace associated with the maximal eigenvalue. A Gram-Schmidt reduction procedure can be used for the computation of Lyapunov exponents in order to identify the eigenelements. Nevertheless, since we are only interested in the maximal eigenvalue of the above matrix, this procedure is not necessary. Concerning the units, the Lyapunov exponents measure the rate at which a system creates or destroys information, and are usually expressed in information per second or per day.

In our study, the local Lyapunov exponents were computed every 0.1-day time step along selected trajectories, with $\Delta = 1$ day (see Figure 9). Note that similar results are obtained for other values of Δ (for instance, $\Delta = 20$ days), and thus are not reported here.

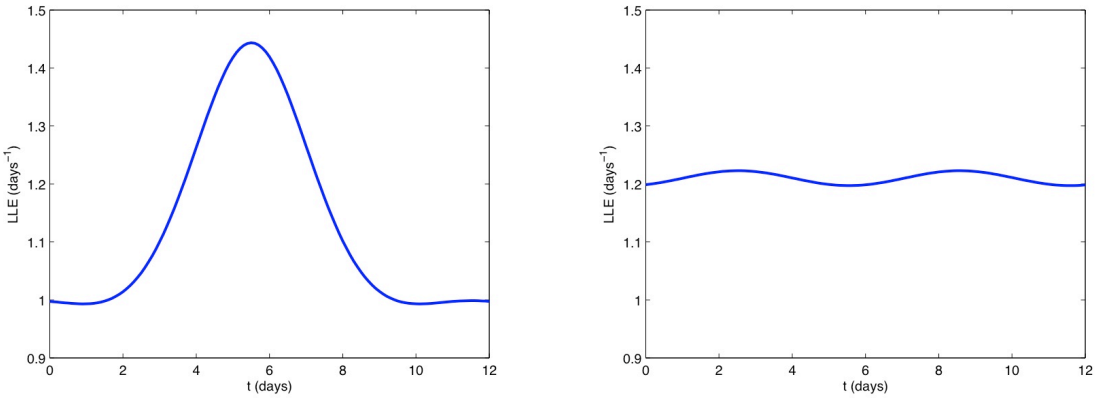

(a) (b)

Figure 9. (a) Local Lyapunov exponent along a halo orbit. (b) Local Lyapunov exponent along an eight-shaped Lissajous orbit.

On Figure 9, LLEs are computed along a halo orbit and an eight-shaped Lissajous orbit of similar energy, around the Lagrange point L_1 in the Earth-Moon system. The first observation that can be done is that in both cases the LLEs are positive. As said before this is in accordance with the chaotic character of the whole system. This means that in both cases nearby trajectories of the periodic orbit may diverge over a certain period of time. However both LLEs behave differently. On the one hand the maximal value of the LLE of the halo orbit is greater than the values of the LLE of the eight-shaped Lissajous orbit, which remains almost constant. On

the other hand, the interval between minimal and maximal values of the LLE of the halo orbit contains the set of values of the LLE of the eight-shaped Lissajous orbit, and the mean values of the LLEs of both orbits seem to be almost the same. This fact can be explained from the following fact: the closer a trajectory gets to a primary (the Moon in this case), the higher its LLE will be. Since the eight-shaped Lissajous orbit is almost vertical, its distance to the primaries remains almost constant during its whole period, and its LLE remains almost constant too. On the contrary, for the same value of energy, the x-excursion of the halo orbit varies a lot (several thousands of kilometers) and hence the orbit gets closer to the Moon. Its LLE varies from a minimal value corresponding to the furthermost point to the Moon, to a maximal value corresponding to the closest point to the Moon. Depending on the energy value, this maximal value gets larger as the orbit gets closer to the Moon. Finally, the stability properties of these periodic orbits are related to their geographic situation. These specificities make that the plots of their LLE versus time are different, but their geographic situation around the same Lagrange point makes that none of them can be said more stable than the other.

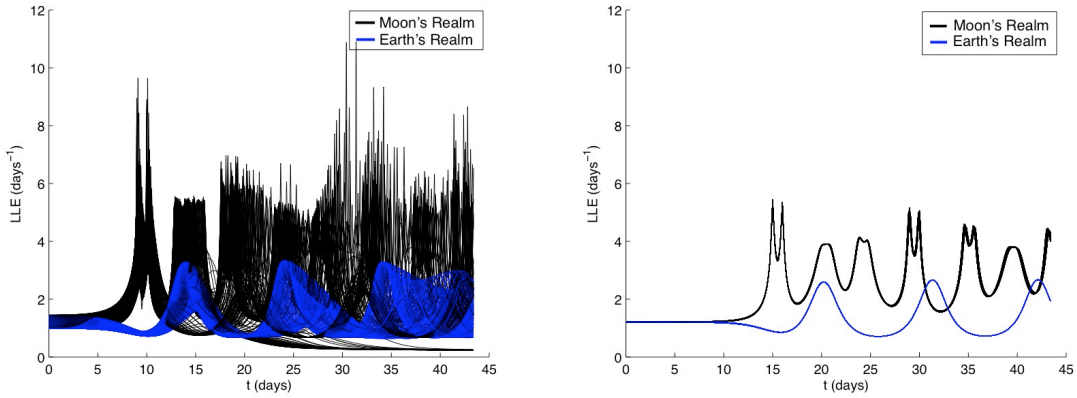

(a) (b)

FIGURE 10. (a) Local Lyapunov exponent of the invariant manifolds of a halo orbit. (b) Local Lyapunov exponents of the invariant manifolds of a eight-shaped Lissajous orbit.

The situation is completely different for their invariant manifolds. On Figure 10, local Lyapunov exponents are computed along the invariant manifolds of the previous halo and eight-shaped Lissajous orbits. The stability difference was not evident concerning the periodic orbits, but this is not the case for their invariant manifolds. In the Earth's realm (in blue on the figure), the LLEs of the invariant manifolds are close for both periodic orbits (by looking closer, the LLEs of the eight-shaped Lissajous orbit manifolds is lower, but the difference is small). In the Moon's realm, the stability difference is evident. The LLEs of the halo orbit manifolds reach 11 days$^{(-1)}$ whereas the LLEs of the eight-shaped Lissajous manifolds take values lower than 5 days$^{(-1)}$ and the difference is similar concerning the mean values. This confirms that some trajectories of the halo orbit manifolds (and the manifolds themselves) are very unstable. As a consequence, predicting the behavior of such a trajectory may happen to be difficult. Things are going differently for the asymptotic trajectories generating the eight-shaped Lissajous manifolds. Their LLEs indicate possible instabilities but, in spite of their small distance to the Moon (which, as mentioned previously, may create instabilities), their LLEs take reasonable values. Notice also that the plot of the LLEs of the eight-shaped Lissajous manifolds has a very smooth

aspect, in contrast with the chaotic aspect of the LLEs of halo orbit manifolds. This is in accordance with the fact that the eight-shaped Lissajous manifolds keep their regular structure of eight-shaped tube even after a large integration time. This nice stability property over large time of the eight-shaped Lissajous manifolds is of potential interest for mission design with low cost.

We stress once again that our simulations lead to similar results for every Lissajous orbit of our one-parameter family of orbits, but we do not claim that the property holds for any possible eight-shaped Lissajous orbit; our current study is prospective, certainly not exhaustive. By the way, the question of deriving rigorously a stability statement, possibly based on the study of some Lyapunov function or something similar, is open.

3.3. Accessible lunar region with the eight-shaped Lissajous invariant manifolds related to the Lagrange point L_1 in the Earth-Moon system

The second interesting property concerning the invariant manifolds of eight-shaped Lissajous orbits is the large accessible lunar region that they cover over large time. By propagating the invariant manifolds of an eight-shaped Lissajous orbit, we observe an oscillating behavior around both primaries. For a given invariant manifold, the part that oscillates around the bigger primary stays rather far from it but the part around the smaller one gets close to it. Our study concerns the Earth-Moon system, and we observe that the part of the invariant manifold in the Earth region stays too far from the Earth to plan a mission using it for a direct departure from the Earth. At the opposite, the part that oscillates around the smaller primary (the Moon) oscillates close to it and thus may be used for a departure or a capture around the Moon (see Figure 11).

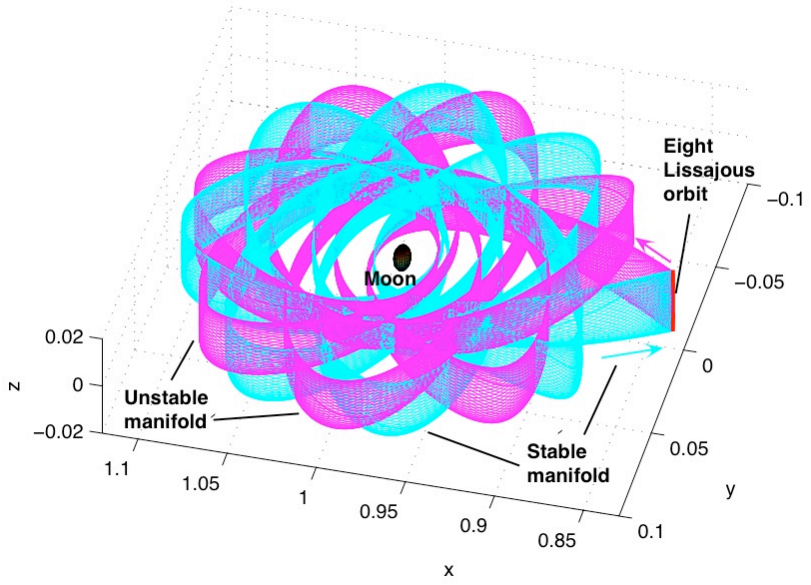

Figure 11. Invariant manifolds of an eight-shaped Lissajous orbit in the neighborhood of the Moon.

The oscillation of these invariant manifolds is not new compared with what can be observed in the classical case of halo orbits. Nevertheless, the constant oscillation of invariant manifolds of eight-shaped Lissajous orbits in the lunar region on the one hand, and the global eight-shaped structure of these manifolds on the other hand, are interesting properties for mission design. Indeed, such invariant manifolds may be used to visit almost all the surface of the Moon, at any time, as shown next. Notice however that, in practice, some other restrictions must be considered,

such as eclipse avoidance, that may cause unfeasibility of the mission (see e.g. [8, 22, 23] for such issues and possible maneuvers).

The idea of using the specific properties of the dynamics around Lagrange points in order to explore lunar regions is far to be new (see e.g. [4, 11, 15, 18, 30, 33]) but has received recently a renewal of interest, in view of new space missions possibly involving a lunar space station (see e.g. [17, 26, 28, 36, 41]).

Lunar strip covered by the invariant manifolds. On Figure 12, we have computed the projection onto the Moon of the invariant manifolds of an eight-shaped Lissajous orbit. We observe that, over a long period, a large surface of the Moon may be scanned, depending on the value of the z-excursion of the orbit.

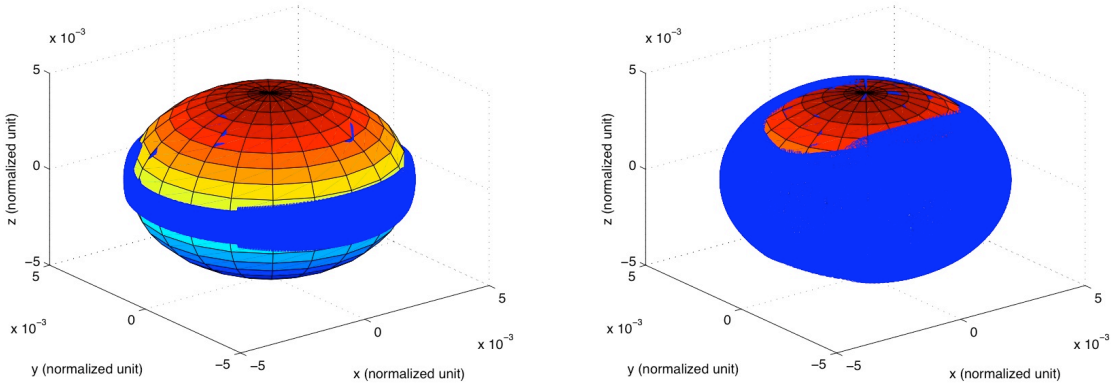

FIGURE 12. Lunar strip covered by the invariant manifolds for (a) Az=10000 km and (b) Az=50000 km.

First, on Figure 12, we observe that, for every value of the z-excursion of the eight-shaped Lissajous orbit, every longitude can be reached. This is due to the oscillation property observed previously. However, this oscillation staying at the equator's level, the latitudes flown over by the manifolds depend on the z-excursion of the eight-shaped Lissajous orbit. If the z-excursion is small, then the latitudes reached are small too. Larger latitudes are reached whenever the z excursion is getting larger. For a z-excursion value equal to 50000 km, and for larger values of the z-excursion, almost all the lunar surface can be scanned from the invariant manifolds. Only the poles cannot be reached directly. A maneuver should be performed to fly over the lunar poles. Anyway, these results show the relevance of invariant manifolds of the eight-shaped Lissajous orbits under consideration to scan almost all the Moon's surface at low cost.

The perigee-angle representation. To complete the previous results, we provide the plot of the invariant manifolds in the perigee-angle plane. For each asymptotic trajectory of the invariant manifolds, the minimal distance to the Moon (perigee) and the corresponding latitude (angle) are computed.

On Figure 13, it is observed that the angles of the perigees range between 20 and 45 degrees. The fact that the range of angles drawn on this figure is smaller than the range of angles covered by the manifolds is not contradictory, since trajectories of invariant manifolds, close to the Moon, reach their closest point to the Moon for a value of inclination between 20 to 45 degrees. Notice that these closest points correspond to positions on the hidden face of the Moon and generally occur at the first oscillation of the manifold around the Moon, i.e, within short time.

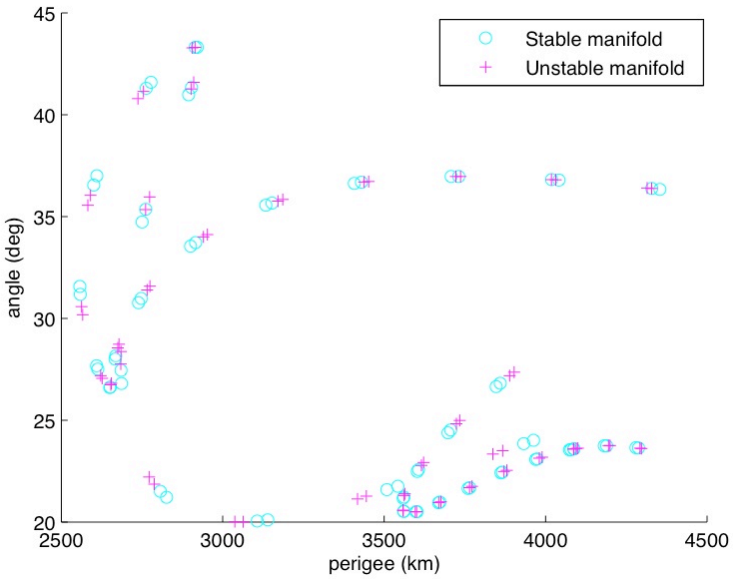

Figure 13. Invariant manifolds of eight-shaped Lissajous orbits in the perigee-angle plane

Figure 13 shows that the minimal distance to the Moon oscillates between 1500 and 5000 kilometers, depending on the z-excursion of the eight-shaped Lissajous orbit (see Table 3.3). The minimal distances are reached after a 9-to-50 days journey from the periodic orbit, but it is clear that for each trajectory 9 days are sufficient to get close enough to the Moon to be captured.

The results about the invariant manifolds oscillating around the Earth are not provided here, since they do not appear to be as relevant as those concerning the Moon. We however mention that the minimal distance between the manifolds of the exterior realm and the Earth oscillate between 115000 and 125000 km, also depending on the value of the z-excursion, with a 40-days journey between the perigee and the eight-shaped Lissajous orbit. This journey duration can be half reduced since similar approach distances are reached after 20 days. In both cases, the corresponding inclinations are meaningless given the large distance between the manifolds and the Earth.

Finally, these results highlight the potential interest of eight-shaped Lissajous orbits (related to the Lagrange point L_1 in the Earth-Moon system) and of their invariant manifolds. Using them, every point located on a circular band around the lunar equator may be reached from the periodic orbit. Except the poles, almost every point of the lunar surface may be flown over from an eight-shaped Lissajous orbit with a large z-excursion.

Conclusion

In this article, we focused on particular periodic orbits around Lagrange points in the circular restricted three-body problem, called eight-shaped Lissajous orbits. A third-order approximation of these orbits has been derived using Lindstedt-Poincaré's method, and families of eight-shaped Lissajous orbits have been computed using a shooting method combined with a continuation method. Then we have shown that eight-shaped Lissajous orbits related to the Lagrange point L_1 in the Earth-Moon system have interesting features. First, their invariant manifolds keep a stable eight-shaped structure over large time, in contrast to the ones of halo orbits. This fact has been put in evidence by computing local Lyapunov exponents. Second, we have shown that

z-excursion of the eight-shaped Lissajous orbit (in km)	Approach time to the Earth (in days)	Approach distance to the Earth (in km)	Approach time to the Moon (in days)	Approach distance to the Moon (in km)
1000	40	116730	43	1673
5000	40	116650	43	1627
10000	40	116800	43	1514
20000	40	117380	9	4502
30000	40	118340	9	5122
40000	40	119670	39	3280
50000	40	121340	42	3333

TABLE 3. Minimal approach time and distance of the manifolds to the Earth and to the Moon in function of the z-excursion of the eight-shaped Lissajous orbit.

invariant manifolds of eight-shaped Lissajous orbits permit to scan almost all the surface of the Moon, depending on the value of the z-excursion. These properties are of potential interest for low cost mission design. Of course such strategies may require a long time transfer and then a compromise has to be found between the energy consumption and the time of transfer. Note also that, having in mind an Earth-Moon mission, invariant manifolds oscillating around the Earth cannot be used directly for a departure from the Earth, due to their too large distance to the Earth. On the contrary, the stability properties of the eight-shaped Lissajous orbits invariant manifolds and the accessibility to the lunar surface provide interesting perspectives, such as easy and economic communications between a spacecraft exploring the Moon and an orbital station based on an eight-shaped Lissajous orbit around the Lagrange point L_1 in the Earth-Moon system. From such an orbital station, almost every point of the Moon may be visited at any time with a low cost.

Bibliography

[1] Abarbanel, H.D.I., Brown, R., Kennel, M.B.: Variation of Lyapunov exponents on a strange attractor. J. Nonlin. Sci. **1**, 175–199 (1991)

[2] Anderson, R.L., Lo, M.W., Born, G.H.: Application of local Lyapunov exponents to maneuver design and navigation in the three-body problem. Paper presented at the AAS/AIAA conference, Big Sky, Montana, AAS 03-569, 3–7 August 2003, http://hdl.handle.net/2014/39457

[3] Arona, L. Masdemont, J.J.: Computation of heteroclinic orbits between normally hyperbolic invariant 3-spheres foliated by 2-dimensional invariant tori in Hill's problem. Discrete Contin. Dyn. Syst. 2007, Dynamical Systems and Differential Equations. Proceedings of the 6th AIMS International Conference, suppl., 64–74 (2007).

[4] Belbruno, E.A., Carrico J.P.: Calculation of weak stability boundary ballistic lunar transfer trajectories. Paper presented at the AAS/AIAA conference, Denver, Colorado, AIAA 2000-4142, August 2000

[5] Benettin, G., Galgani, L., Giorgilli, A., Strelcyn J.-M.: Lyapunov characteristic exponents for smooth dynamical systems and for hamiltonian systems; a method for computing all of them. Part 1: Theory, and Part 2: Numerical Application. Meccanica **15**, 9–30 (1980)

[6] Bonnard, B., Faubourg, L., Trélat, E.: Mécanique céleste et contrôle des véhicules spatiaux. Math. & Appl. **51**, Springer Verlag (2006)

[7] Breakwell, J.V., Brown, J.V.: The halo family of 3-dimensional of periodic orbits in the Earth-Moon restricted 3-body problem. Celestial Mechanics **20**, 389–404 (1979)

[8] Canalías, E.,Gómez, G., Marcote, M., Masdemont, J.J.: Assessment of mission design including utilization of libration points and weak stability boundaries. ESA publication (electronic). Ariadna id: 03/4103. ESA contract number 18142/04/NL/MV Final report (2004)

[9] Dellnitz, M., Padberg, K. , Post, M., Thiere, B.: Set oriented approximation of invariant manifolds: review of concepts for astrodynamical problems. In: New trends in astrodynamics and applications III, AIP Conference Proceedings **886**, 90–99 (2007)

[10] Dieci, L., Russell, R.D., Van Vleck, E.S.: On the computation of Lyapunov exponents for continuous dynamical systems. SIAM J. Numer. Anal. **34**(1), 402–423 (1997)

[11] Dunham, D.W., Farquhar, R.W.: Libration Points Missions. In: International Conference on Libration Points and Applications, Girona, Spain, 10-14 June 2002

[12] Eckhardt, B., Yao, D.M.: Local Lyapunov exponents in chaotic systems. Phys. D **65**(1-2), 100–108 (1993)

[13] Euler, L.: De motu rectilineo trium corporum se mutuo attrahentium. Novi commentarii academiae scientarum Petropolitanae **11**, 144–151 (1767). In: Oeuvres, Seria Secunda tome XXv Commentationes Astronomicae.

[14] Farquhar, R.W.: Station-keeping in the vicinity of collinear libration points with an application to a Lunar communications problem. Space Flight Mechanics, Science and Technology Series **11**, 519–535 (1966)

[15] Farquhar, R.W.: The utilization of Halo orbits in advanced lunar operations. Technical Report X-551-70-449, Goddard Space Flight Center, Maryland (1970)

[16] Farquhar, R.W.: A halo-orbit lunar station. Astronautics & Aeronautics **10**(6), 59–63 (1972)

[17] Farquhar, R.W., Dunham, D.W., Guo, Y., McAdams J.V.: Utilization of libration points for human exploration in the Sun-Earth-Moon system and beyond. Acta Astronautica **55**(3-9), 687–700 (2004)

[18] Gómez, G., Koon, W.S., Lo, M.W., Marsden, J.E., Masdemont, J., Ross, S.D.: Invariant manifolds, the spatial three-body problem and space mission design. Adv. Astronaut. Sci. **109**, 3–22 (2001)

[19] Gómez, G., Koon, W.S., Lo, M.W., Marsden, J.E., Masdemont, J., Ross, S.D.: Connecting orbits and invariant manifolds in the spatial three-body problem. Nonlinearity **17**, 1571–1606 (2004)

[20] Gómez, G., Masdemont, J., Simó, C.: Lissajous orbits around halo orbits. Adv. Astronaut. Sci. **95**, 117–34 (1997)

[21] Gómez, G., Masdemont, J., Simó, C.: Quasihalo orbits associated with libration points. J. Astronaut. Sci. **46**, 135–76 (1998)

[22] Gómez, G., Llibre, J., Martinez, R., Simó, C.: Dynamics and mission design near libration points, Volumes I, II (Fundamentals: The Case of Collinear Points; Advanced Methods for Collinear Points, resp.), World Scientific Monograph Series in Mathematics, Volumes I, II (2001)

[23] Gómez, G., Jorba, A., R., Simó, C., Masdemont, J.J.: Dynamics and mission design near libration points. Volumes III, IV (Advanced methods for collinear points; Advanced methods for triangular points, resp.), World Scientific Monograph Series in Mathematics, Volumes III, IV (2001)

[24] Howell, K.C., Pernicka, H.J.: Numerical determination of Lissajous orbits in the restricted three-body problem. Celestial Mechanics **41**, 107–124 (1988)

[25] Jorba, A., Masdemont, J.: Dynamics in the center manifold of the collinear points of the restricted three-body problem. Physica D **132**, 189–213 (1999)

[26] Koon, W.S., Lo, M.W., Marsden, J.E., Ross, S.D.: Dynamical Systems, the three-body problem and space mission design. Springer (2008)

[27] Lagrange, J.-L.: Essai sur le problème des trois corps. Prix de l'académie royale des Sciences de paris, tome IX (1772). In: Oeuvres de Lagrange **6**, Gauthier-Villars, Paris, 272–282 (1873).

[28] Lo, M.W., Chung, M.J.: Lunar sample return via the interplanetary highway. Paper presented at the AIAA/AAS Astrodynamics Specialist Conference and Exhibit, Monterey, California, 5–8 August 2002, AIAA 2002-4718

[29] Lyapunov A.M.: The general problem of the stability of motion. Comm. Soc. Math. Kharkow (1892) (in Russian), reprinted in English, Taylor & Francis, London, 1992

[30] Marsden, J.E., Koon, W.S., Lo, M.W., Ross, S.D.: Low energy transfer to the Moon. Celestial Mechanics Dyn. Astron. **81**, 27–38 (2001)

[31] Masdemont, J.J.: High order expansions of invariant manifolds of libration point orbits with applications to mission design. Dyn. Syst. **20**(1), 59–113 (2005)

[32] Meyer, K.R., Hall, G.R.: Introduction to Hamiltonian dynamical systems and the N-body problem. Applied Math. Sci. **90**, Springer-Verlag, New-York (1992)

[33] Miller J.K., Belbruno E.A.: Sun-perturbated Earth-to-Moon transfers with ballistic capture. J. Guidance, Control Dynam. **16**(4), 770–775 (1993)

[34] Moser, J.: On the generalization of a theorem of A. Lyapunov. Commun. Pure Appl. Math. **11**, 257–271 (1958)

[35] Oseledec, V. I.: A multiplicative ergodic theorem. Characteristic Ljapunov, exponents of dynamical systems. (Russian) Trudy Moskov. Mat. Obsc. **19**, 179–210 (1968)

[36] Renk, F., Hechler, M., Messerschmid, E.: Exploration missions in the Sun-Earth-Moon system: a detailed view on selected transfer problems. Acta Astronautica, in Press (2009)

[37] Richardson, D.L.: Analytic construction of periodic orbits about the collinear points. Celestial mechanics **22**, 241–253 (1980)

[38] Szebehely, V.G.: Theory of orbits: the restricted problem of three bodies. Academic Press, New-York (1967)

[39] Wolf, A., Swift, J.B., Swinney, H.L., Vastano, J.A.: Determining Lyapunov exponents from a time series. Physica **16D**, 285–317 (1985)

[40] Wolff, R.C.L.: Local Lyapunov exponents: looking closely at chaos. J. Roy. Statist. Soc. Ser. B **54**(2), 353–371 (1992)

[41] Yazdi, K., Messerschmid, E.: A lunar exploration architecture using lunar libration point one. Aerospace Science and Technology **12**, 231–240 (2008)